

NEWTON MAPS: FRACTALS FROM NEWTON'S METHOD FOR THE CIRCLE MAP

JULYAN H. E. CARTWRIGHT

Institut de Bioenginyeria, Universitat Miguel Hernández,

E-03550 Sant Joan d'Alacant, Spain

Email julyan@hp1.uib.es, WWW <http://formentor.uib.es/~julyan>

Computers and Graphics, **23**, 607–612, 1999

Abstract

To understand why two interacting oscillators synchronize with each other, or lock together and resonate at some rational frequency ratio, dynamical-systems theory shows that one should study circle maps and their periodic orbits. One can easily explore the structure of these periodic orbits using Newton maps, derived from Newton's method for finding the roots of an equation. I present here some interesting and beautiful examples of fractals encountered in Newton maps while investigating the periodic orbits of circle maps.

1 Introduction

In 1665, Christiaan Huygens made a serendipitous discovery. Working on a military project to develop better time-keeping at sea, he had two pendulum clocks in his laboratory — very expensive pieces of hardware destined for Dutch warships — hanging from a pole slung across the backs of two chairs. He noted [1] that over a period of half an hour or so, the two pendulums tended to lock into step with each other.

He called his discovery the sympathy of clocks. Today, it is known as locking, resonance, or synchronization in oscillators, and is an enormously important part of dynamical-systems theory that has applications to physics, chemistry, biology, engineering, in fact to any place where there is something that oscillates. The theory of dynamical systems allows one to investigate synchronization by showing that the behaviour of complex oscillating systems like pendulum clocks is described by simple equations called circle maps.

The sine circle map

$$\theta_{m+1} = \theta_m + \Omega - \frac{k}{2\pi} \sin 2\pi\theta_m \pmod{1} \quad (1)$$

is a one-dimensional discrete mapping that describes how an oscillator of natural frequency Ω behaves when coupled to another of frequency one by a coupling of strength k . When $k = 0$ the oscillator runs uncoupled at frequency Ω , but when $k > 0$ it can lock into a periodic orbit: a resonance with some rational ratio p/q to the driving frequency. To measure the average rotation per iteration of the map — the frequency of the oscillator — it is useful to define the

rotation number [2]

$$\rho(\theta) = \lim_{m \rightarrow \infty} \frac{\theta_m - \theta_0}{2\pi m}. \quad (2)$$

Keeping k constant, we can iterate the circle map for values of Ω between 0 and 1, and plot rotation number ρ against Ω . Luckily, it is not necessary to iterate to infinity; the first few iterations can be discarded to remove transient effects, and a few hundred iterations are then sufficient to give an accurate value for ρ . This plot has been termed the devil's staircase; the stairs are lockings: periodic orbits with different rational rotation numbers that show up as flat steps as in Fig. 1. When $k < 1$ the map is called subcritical, and intervals on which the rotation number is constant and rational, where there is a periodic orbit of a particular period, punctuate intervals of increasing rotation number, whereas in supercritical circle maps ($k > 1$) the periodic orbits overlap. But in a critical circle map at $k = 1$, the staircase is complete; at every value of Ω there is a periodic orbit, and the rotation number increases in a staircase fashion with steps at each rational rotation number and risers in between. The staircase has an infinity of steps at all scales so that someone climbing the staircase step by step would never reach the top — a devilish construction indeed! The devil's staircase becomes the devil's quarry illustrated in Fig. 1 when we look at the picture in terms of the nonlinearity k as well as the forcing frequency Ω , so that we have rotation number ρ represented by height in a three-dimensional quarry. The size of the step decreases as the period of the associated cycle increases. Between any two steps p/q and p'/q' associated with rational rotation numbers, the largest intermediate step is given by the rational number having the smallest denominator in that interval. This ordering of periodic

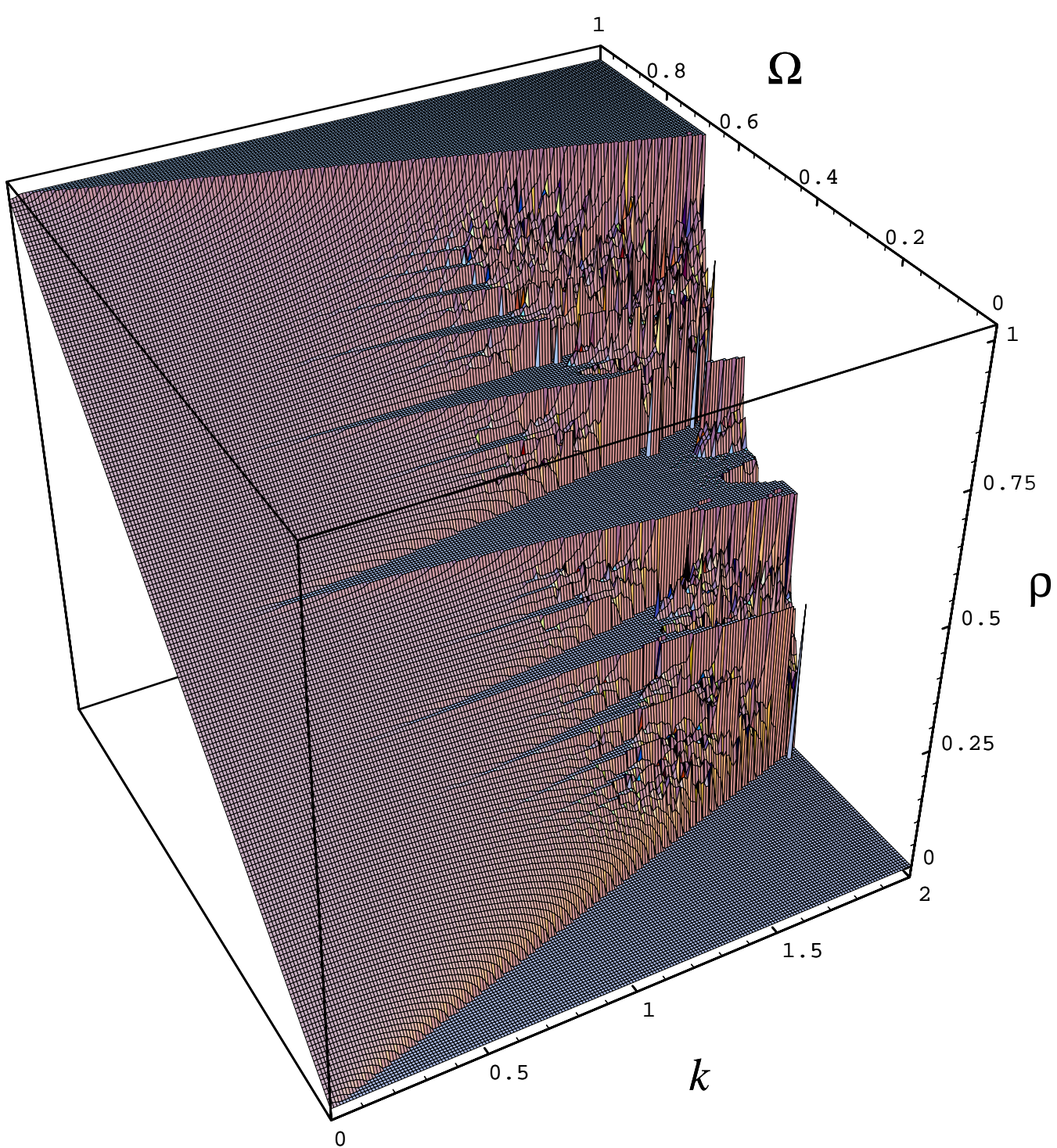


Figure 1: The devil's quarry in the sine circle map for $0 < \Omega < 1$ and $0 < k < 2$. The periodic orbits, the steps in the quarry, are sized according to the Farey rule (3). The devil's staircase is a section front to back (k constant) through the quarry. The steps are often called Arnold tongues after the mathematician V. I. Arnold.

orbits is provided by the Farey tree [3, 4, 5, 6] constructed using the Farey mediant

$$\frac{p}{q} \oplus \frac{p'}{q'} = \frac{p+p'}{q+q'}. \quad (3)$$

To obtain the Farey tree with this rule we start with the two ends of the unit interval written as $0/1$ and $1/1$, to produce the ordering at the first level $1/2$, at

the second level $1/3$ and $2/3$, at the third level $1/4$, $2/5$, $3/5$, and $3/4$, and so on. We can see this ordering of periodic orbits reflected in the sizes of the steps in Fig. 1.

There are many other fascinating phenomena in the circle map, for example, chaos is found in the supercritical circle map as iterates wander between the overlapping resonances; this is seen in the devil's

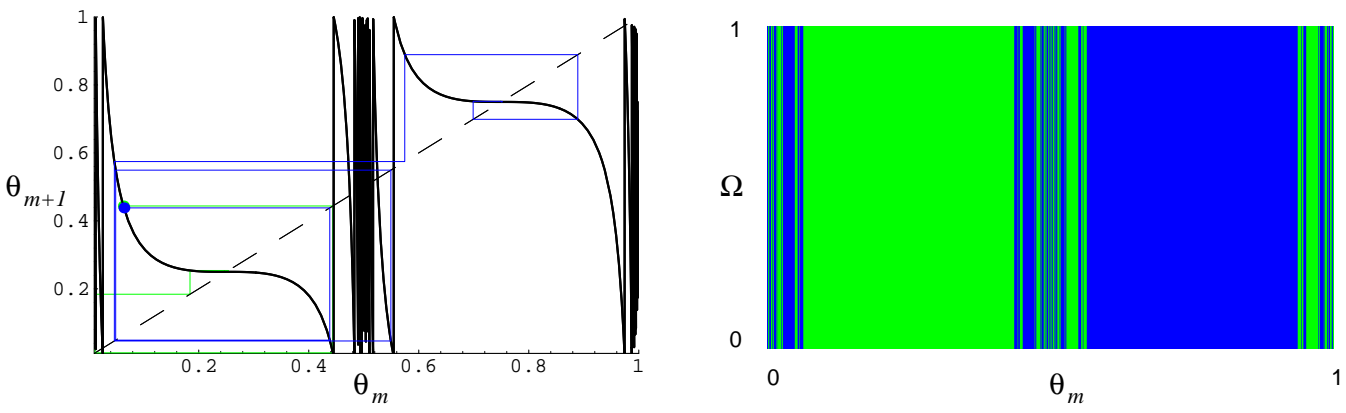


Figure 2: (a) Two trajectories in the Newton map $\theta_{m+1} = \theta_m + 1/(2\pi) \cot 2\pi\theta_m \pmod{1}$, that is (14) with $c = 1$, showing sensitive dependence on initial conditions. The trajectory started at 0.063 ends up in one basin of attraction; that starting at 0.064 finishes in the other basin. (b) Fractal structure in the basins of attraction of the two fixed points.

quarry of Fig. 1 as the jagged rock face for $k > 1$ [7]. Here, though, I shall concentrate on the periodic orbits.

2 Newton Maps

To study the Farey ordering of the periodic orbits we have to be able to locate with great precision where they begin and end. To do this we can use the method Newton invented for finding the roots (zeroes) of a function $g(x)$

$$\mathbf{x}_{m+1} = \mathbf{x}_m - (J^{-1}(\mathbf{x}_m))g(\mathbf{x}_m), \quad (4)$$

where J is the Jacobian matrix of $g(x)$. We want to find periodic orbits p/q of the sine circle map

$$f(\theta) = \theta + \Omega - \frac{k}{2\pi} \sin 2\pi\theta \pmod{1}, \quad (5)$$

where $f^q(\theta) = \theta$. We wish to locate the boundary points of these periodic orbits where

$$\frac{\partial f^q(\theta)}{\partial \theta} = c = 1. \quad (6)$$

If we wanted to look at other aspects of the periodic orbits, we could also find the superstable points for $c = 0$, or the period doubling points at which $c = -1$, so we will do the analysis for general c . Using Newton's method we wish to have

$$f^q(\theta) - \theta - p = 0, \quad \frac{\partial f^q(\theta)}{\partial \theta} - c = 0. \quad (7)$$

We let

$$g = \left[f^q(\theta) - \theta - p, \frac{\partial f^q(\theta)}{\partial \theta} - c \right], \quad (8)$$

and use Newton's method to find the roots of g .

The Newton maps that are produced quickly become mathematically complex as the period of the

orbit increases. To give a simple example I shall look first at the period-one (i.e., $q = 1$) or fixed points in the circle map, at which $\Omega - k/(2\pi) \sin 2\pi\theta = 0 \pmod{1}$. In this case we have

$$g = \left[\Omega - \frac{k}{2\pi} \sin 2\pi\theta - p, 1 - k \cos 2\pi\theta - c \right]. \quad (9)$$

We can locate the period-one orbits either along lines of fixed k , varying Ω , or along lines of fixed Ω , varying k . I shall analyse the Newton maps produced by each of the two cases in turn.

3 The Period-One $[\theta, \Omega]$ Newton Map

Let us look at the Newton map of period-one (fixed) points in the sine circle map using θ and Ω as variables ($\mathbf{x} = [\theta, \Omega]$). The Jacobian is

$$J = \begin{bmatrix} -k \cos 2\pi\theta & 1 \\ 2\pi k \sin 2\pi\theta & 0 \end{bmatrix}, \quad (10)$$

which from (4) gives us the Newton map

$$\begin{aligned} \theta_{m+1} &= \theta_m + \frac{1}{2\pi} \left(\cot 2\pi\theta_m + \frac{c-1}{k} \operatorname{cosec} 2\pi\theta_m \right), \\ \Omega_{m+1} &= p + \frac{k}{2\pi} \left(\operatorname{cosec} 2\pi\theta_m + \frac{c-1}{k} \cot 2\pi\theta_m \right). \end{aligned} \quad (11)$$

Despite appearances, this is a one-dimensional map, since θ_{m+1} and Ω_{m+1} depend only on θ_m , and not on Ω_m .

The fixed points $[\theta_{fp}, \Omega_{fp}]$ of the Newton map are at

$$\left[n + \frac{\alpha_1}{2\pi}, p + \frac{1}{2\pi} \sqrt{k^2 - (1-c)^2} \right], \quad n \in \mathbb{Z}, \quad (12)$$

and

$$\left[n + \frac{\alpha_2}{2\pi}, p - \frac{1}{2\pi} \sqrt{k^2 - (1-c)^2} \right], \quad n \in \mathbb{Z}, \quad (13)$$

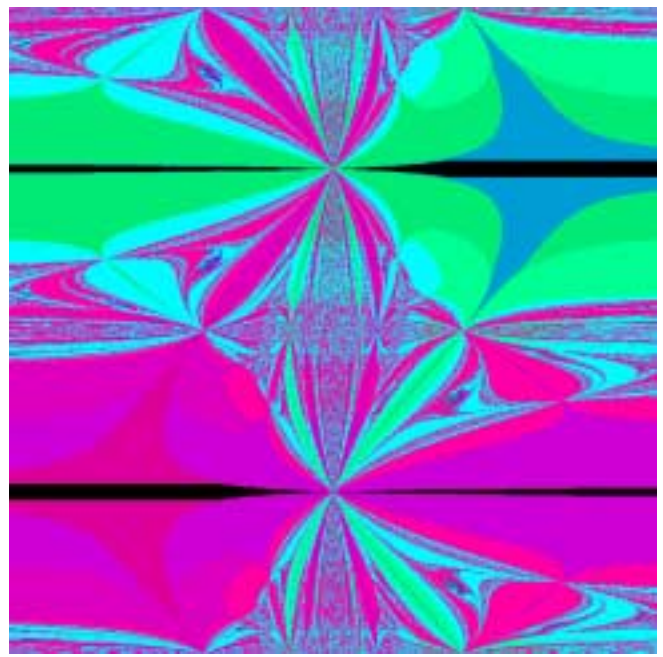
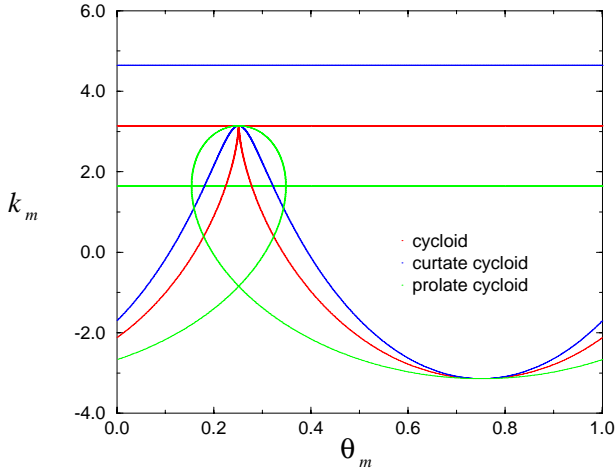


Figure 3: (a) Cycloids produced by iterating once three lines of constant k in the map. That for $k < k_{max}$ gives a curtate cycloid, like a point within the circumference of a rolling wheel; that for $k = k_{max}$ gives an ordinary cycloid, as a point on the circumference of the wheel; and for $k > k_{max}$ there is a prolate cycloid, like a point outside the rolling circumference — a flange on a train wheel, for instance. (b) The map (16) with parameters $\Omega = 0.5$, $p = 0$, $c = 1$. The ordinate is $0 < \theta < 1$, and the abscissa $-5 < k < 5$. The basins of attraction of the fixed points $[\theta_{fp}, k_{fp}]$ at $[1/4, \pi]$ and $[3/4, -\pi]$ are depicted in shades of crimson and turquoise; the darker tones represent more rapid approach to the fixed points.

where α_1 and α_2 are the two values of $\arccos((1-c)/k)$ in the range $[0, 2\pi)$. Of course if $|k| < |1-c|$ then there are no fixed points.

If, as is often the case, we are interested only in finding Ω values, whatever the value of θ , we may lump together all the fixed points with $\Omega_{fp} = p+1/(2\pi)\sqrt{k^2 - (1-c)^2}$ and all the others with $\Omega_{fp} = p-1/(2\pi)\sqrt{k^2 - (1-c)^2}$. In this way we are left with only two fixed points. This procedure is equivalent to putting the map on the unit circle, that is looking at the fixed points of the map

$$\theta_{m+1} = \theta_m + \frac{1}{2\pi} \left(\cot 2\pi\theta_m + \frac{c-1}{k} \operatorname{cosec} 2\pi\theta_m \right) \bmod 1. \quad (14)$$

By virtue of its infinitely many branches, illustrated in Fig. 2(a), this map has the fractal structure shown in Fig. 2(b) of the boundaries of the basins of attraction of the fixed points. At the edges of the large contiguous regions around the two fixed points, computer investigation reveals structure at finer and finer scales.

4 The Period-One $[\theta, k]$ Newton Map

Now let us look at the Newton map produced by using θ and k as variables ($\mathbf{x} = [\theta, k]$). The Jacobian

is

$$J = \begin{bmatrix} -k \cos 2\pi\theta & -1/(2\pi) \sin 2\pi\theta \\ 2\pi k \sin 2\pi\theta & -\cos 2\pi\theta \end{bmatrix}, \quad (15)$$

giving us the Newton map

$$\begin{aligned} \theta_{m+1} &= \theta_m + 1/(2\pi k_m) (2\pi(\Omega - p) \cos 2\pi\theta_m \\ &\quad + (c-1) \sin 2\pi\theta_m), \\ k_{m+1} &= 2\pi(\Omega - p) \sin 2\pi\theta_m - (c-1) \cos 2\pi\theta_m. \end{aligned} \quad (16)$$

This map, in contrast to the previous one, is two-dimensional, but since $\theta_{m+1} = f(\theta_m, k_m)$ and $k_{m+1} = g(\theta_m, k_m)$, a set of points with the same θ will map to a set with the same k . We can write the map as

$$\begin{aligned} \theta_{m+1} &= \theta_m + R/(2\pi k_m) \sin(2\pi\theta_m + \alpha), \\ k_{m+1} &= R \cos(2\pi\theta_m + \alpha), \end{aligned} \quad (17)$$

where

$$R = \sqrt{(c-1)^2 + [2\pi(\Omega - p)]^2} \quad (18)$$

and

$$\alpha = \arctan \frac{2\pi(\Omega - p)}{c-1}. \quad (19)$$

Let us call the two values of this arctangent in the range $[0, 2\pi)$ α_1 and α_2 . It is now easy to see that the map is bounded in k with maximum $|k_{m+1}| = R = |k_{max}|$.

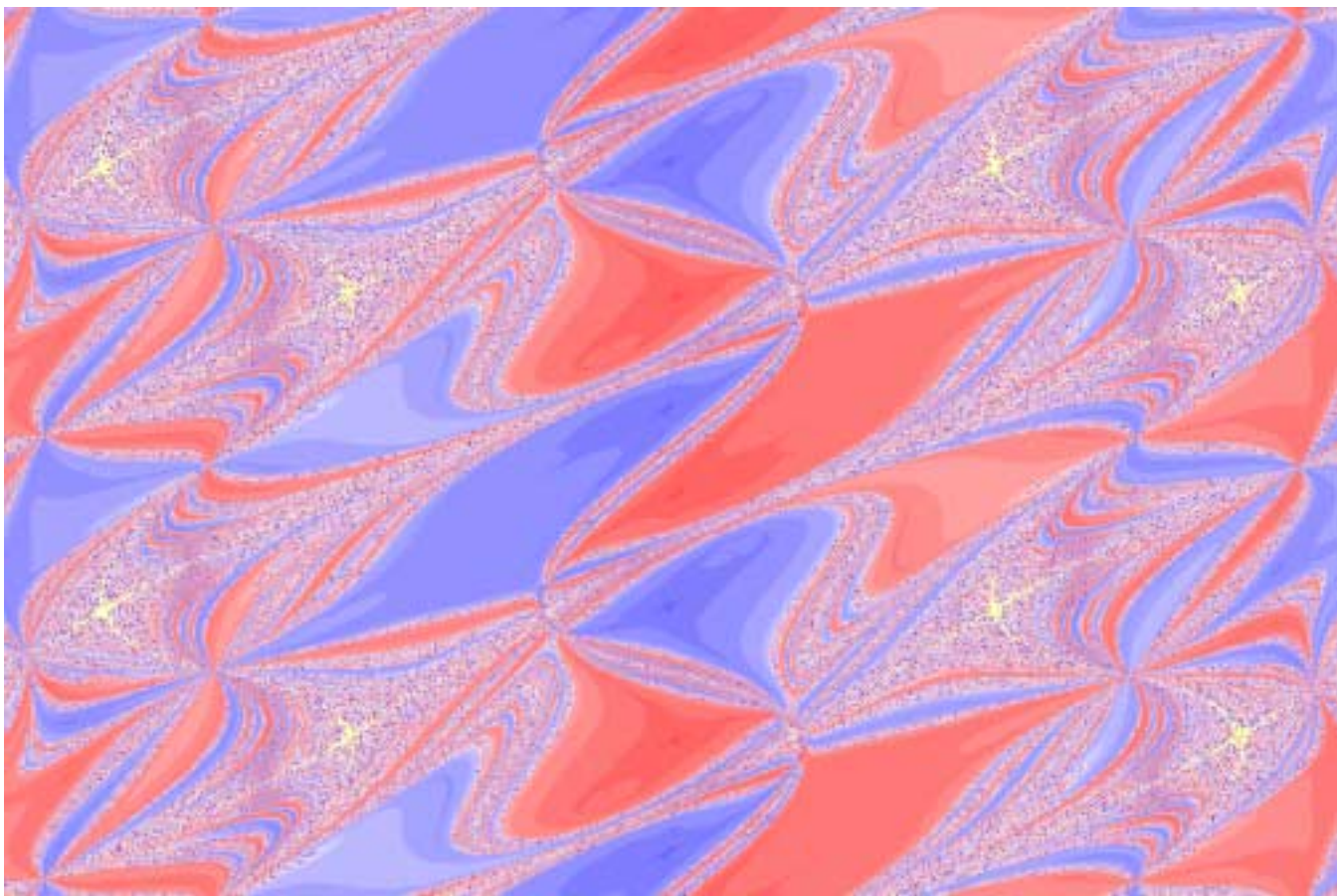


Figure 4: Basins of attraction for a Newton map finding the edges of the $1/2$ tongue in a subcritical $k = 1/2$ sine circle map; the boundaries of the plot are $-0.5 < \theta < 1.5$ for the ordinate, and $-1 < \Omega < 2.0$ for the abscissa. Red and blue represent the basins of the two fixed points that arise from finding the two edges of the tongues. The deeper the colour, the faster is the approach to the basin from that point. The yellow points are where the trajectory failed to fall into either basin within twenty iterations.

It is interesting to note that if we set $\phi = 2\pi\theta_m + \alpha$, $x = 2\pi\theta_{m+1} + \alpha$, $y = 1 - k_{m+1}/k_m$ and $b = R/k_m$ we obtain

$$\begin{aligned} x &= \phi + b \sin \phi, \\ y &= 1 + b \cos \phi, \end{aligned} \quad (20)$$

which are the parametric equations for a cycloid, the curve traced out by a point on a wheel being rolled along a flat surface. A curtate cycloid is obtained when $|b| < 1$, an ordinary cycloid has $|b| = 1$ and a prolate cycloid is given when $|b| > 1$. We have $b = R/k_m$, so lines of constant k_m in the map iterate to different cycloids with $|k_m| = R = k_{max}$ being the changeover point; see Fig. 3(a).

The map has fixed points $[\theta_{fp}, k_{fp}]$ at

$$[n - \alpha_1/(2\pi), R], \quad [n - \alpha_2/(2\pi), -R], \quad n \in \mathbb{Z}. \quad (21)$$

Note that points with any k except the singular value $k = 0$ with the same θ -value as a fixed point map straight into it. That is

$$[\theta_{fp} + n/2, k], \quad k \neq 0, \quad n \in \mathbb{Z}, \quad (22)$$

iterates to $[\theta_{fp}, k_{fp}]$. Thus there exists an infinity of preimages of each fixed point. The map also has a singular line at $k = 0$. By the same reasoning as above, there exists an infinity of preimages of points on the singular line.

$$[\theta_{fp} + n/2 + 1/4, k], \quad k \neq 0, \quad n \in \mathbb{Z}, \quad (23)$$

iterates to $[\theta, 0]$, somewhere on the singular line and

$$[\theta_{fp} + n/2 + 1/4, \pm R/((n + 1/2)\pi)], \quad n \in \mathbb{Z} \quad (24)$$

iterates to $[\theta_{fp}, 0]$, on the singular line below a fixed point. All this interesting behaviour may be observed in Fig. 3(b), showing the basins of attraction of the fixed points.

5 Periods Two and Higher

The mappings are no longer one-dimensional, and their structures are even more complex than those described above. In the (θ, Ω) Newton map for periods two and higher there are two fixed points, corresponding to the two sides of the Arnold tongues in

Fig. 1, and colouring their basins of attraction differently in an image, together with a third colour for points that do not converge to either solution in a certain number of iterations, shows the complexity that exists, as I illustrate in Fig. 4. This image from my doctoral thesis [8], was used for the cover of Volume 5 of the journal *Nonlinearity*.

6 Further Ideas

I have shown some of the beautiful dynamical structures that can be found in Newton maps of the circle map. The idea can be carried further by iterating the process: one can make Newton maps of Newton maps of the circle map, Newton maps of Newton maps of . . . , and so on recursively. But that story will have to wait for another time.

References

[1] C. Huygens. Extrait d'une lettre écrite de La Haye, le 26 fevrier 1665. *Journal des Scavans*, (11 (16 March)), 1665. See the correction published in the following issue: Observation a faire sur le dernier article de precedent journal, où il est parlé de la concordance de deux pendules suspenduës à trois ou quatre pieds l'une de l'autre. *Journal des Scavans*, (12 (23 March)), 1665. Huygens' notebook is reprinted in *Œuvres Complètes de Christiaan Huygens*, volume 17, page 185, Société Hollandaise des Sciences, 1888–1950. A good historical perspective is provided by J. G.

Yoder. *Unrolling Time—Christiaan Huygens and the Mathematization of Nature*. Cambridge University Press, 1988.

- [2] D. K. Arrowsmith and C. M. Place. *An Introduction to Dynamical Systems*. Cambridge University Press, 1990.
- [3] D. L. González and O. Piro. Chaos in a nonlinear driven oscillator with exact solution. *Physical Review Letters*, **50** 870–872, 1983.
- [4] D. G. Aronson, M. A. Chory, G. R. Hall, and R. P. McGehee. Bifurcations from an invariant circle for two-parameter families of maps of the plane: A computer-assisted study. *Communications in Mathematical Physics*, **83** 303–354, 1983.
- [5] P. Cvitanović, B. Shraiman, and B. Söderberg. Scaling laws for mode lockings in circle maps. *Physica Scripta*, **32** 263–270, 1985.
- [6] B.-L. Hao. *Elementary Symbolic Dynamics and Chaos in Dissipative Systems*. World Scientific, 1989.
- [7] D. K. Arrowsmith, J. H. E. Cartwright, A. N. Lansbury, and C. M. Place. The Bogdanov map: bifurcations, mode locking, and chaos in a dissipative system. *International Journal of Bifurcation and Chaos*, **3** 803–842, 1993.
- [8] J. H. E. Cartwright. *Chaos in Dissipative Systems: Bifurcations and Basins*. PhD thesis, Queen Mary and Westfield College, University of London, 1992.